DOI:
10.1161/ATVBAHA.111.239046

Document Version
Peer reviewed version

Author Disclosures

Daxin Chen: No disclosures

Seema Shrivastava: No disclosures

Liang Ma: No disclosures

El Li Tham: No disclosures

Joel Abrahams: No disclosures

J. David Coe: No disclosures

Diane Scott: No disclosures

Robert I Lechler: No disclosures

John H McVey: No disclosures

Anthony Dorling: No disclosures

Inhibition of thrombin receptor signalling on α-smooth muscle actin$^+$ CD34$^+$ progenitors leads to repair after murine immune vascular injury.

Chen – Repair by PAR-1 inhibition on myeloid progenitors

D. Chen PhD,[1] S. Shrivastava PhD,[1,2] L. Ma,[1] E-L Tham,[1] J. Abrahams BSc,[2] J. D. Coe BSc, [2] D. Scott PhD, [2] R. I. Lechler PhD FRCP,[1] J. H. McVey PhD,[3] A. Dorling PhD FRCP[1]

[1] Medical Research Council (MRC) Centre for Transplantation, King's College London, King's Health Partners, Guy's Hospital, Great Maze Pond, London UK SE1 9RT

[2] Department of Immunology, Imperial College London, Hammersmith Hospital, Du Cane Road, London, UK W12 0NN

[3]Thrombosis Research Institute, Manresa Road, London, UK. SW3 6LR

Corresponding Author: Prof. Anthony Dorling, MRC Centre for Transplantation, King's College London, Guy's Hospital, London, UK SE1 9RT

Tel +44 (0)20 7188 5880 Fax +44 (0)20 7188 5660

Email; anthony.dorling@kcl.ac.uk

Word count body:	5623 in figure legends
Word count abstract:	203
Total figures:	5 (+4 online supplementary)
Total tables:	1 (+2 online supplementary)

Abstract

Objective: To use mice expressing human tissue factor pathway inhibitor (hTFPI) on α-smooth muscle actin (SMA)$^+$ cells as recipients of allogeneic aortas to gain insights into the cellular mechanisms of intimal hyperplasia (IH).

Methods and Results: BALB/c aortas (H-2^d) transplanted into α-TFPI-Tg mice (H-2^b) regenerated a quiescent endothelium in contrast to progressive IH seen in C57BL/6 wild-type (WT) mice even though both developed aggressive anti-H-2^d alloresponses, indicating similar vascular injuries. Adoptively transferred Tg CD34$^+$ (but not CD34$^-$) cells inhibited IH in WT recipients, indicating the phenotype of α-TFPI-Tg mice was due to these cells. Compared to syngeneic controls, endogenous CD34$^+$ cells were mobilized in significant numbers after allogeneic transplantation, the majority showing sustained expression of tissue factor (TF) and protease-activated receptor-1 (PAR-1). In WT, most were CD45$^+$ myeloid progenitors co-expressing CD31, VEGFR-2 and E-selectin; 10% of these cells co-expressed α-SMA and were recruited to the neointima. In contrast, the α-SMA$^+$ hTFPI$^+$ CD34$^+$ cells recruited in Tg recipients were from a CD45$^-$ lineage. WT CD34$^+$ cells incubated with a PAR-1 antagonist or taken from PAR-1-deficient mice inhibited IH like Tg cells.

Conclusions: Specific inhibition of thrombin generation or PAR-1 signalling on α-SMA$^+$ CD34$^+$ cells inhibits IH and promotes regenerative repair despite ongoing immune-mediated damage.

Key words: Coagulation, Immune system, Thrombin, Transplantation, Vascular Biology

Intimal hyperplasia (IH) developing after immune-mediated injury is associated with vascular remodelling, progressive loss of lumen and chronic ischaemia of downstream tissues. This process underpins chronic rejection after transplantation, in which the injury is mediated by the alloimmune response.

The precise cellular mechanisms by which IH develops are not clearly understood. A commonly accepted model proposes that T cells and macrophages infiltrating the tunica intima and adventitia [1, 2] make cytokines that induce changes in medial vascular smooth muscle cells (SMC), causing them to migrate, proliferate and become 'modulated' SMC characteristically seen in IH [3]. Interferon gamma (IFNγ) emerges as an important cytokine influencing SMC phenotype in this model [4].

Data from rodent models of transplant arteriosclerosis (TA) [5-7] indicate that a significant proportion of alpha smooth muscle actin (α-SMA)-expressing neointimal cells are recipient-derived. Although labelled 'SMC' by some authors, recent data indicates these cells are inflammatory leukocytes, lacking expression of markers of a 'true' SMC lineage such as myosin heavy chain and calponin [8]. The role and importance of these recipient α-SMA$^+$ leukocytes in the pathogenesis of IH is unknown.

Our previous work partly addressed this. We examined bone marrow (BM)-derived α-SMA$^+$ cells following mechanical endoluminal injury [9-11]. Tissue factor (TF)-initiated thrombin generation and protease activated receptor-1 (PAR-1) stimulation on these cells was necessary for IH to develop. Transgenic mice expressing an anticoagulant fusion protein based on human tissue factor pathway inhibitor (hTFPI) under the control of a modified α-SMA promoter ("α-TFPI-Tg" mice) failed to develop the IH seen in wild-type (WT) mice. Instead, the neointima contained α-SMA$^+$ hTFPI-expressing cells covered by a quiescent endothelium; i.e. the arteries were repaired back to a pre-injured state. BM chimera and adoptive transfer experiments showed that repair was dependent on transgene expression by CD34$^+$ cells [9]. Additionally, inhibition of PAR-1 on transferred CD34$^+$ cells induced the

same phenotype [10]. In an attempt to understand neointima formation in WT mice, we showed that thrombin induced proliferation, inhibited apoptosis and promoted the dominant outgrowth of a minority population of circulating α-SMA$^+$CD34$^+$ cells (accounting for approximately 3% of all circulating CD34$^+$ cells) which had a phenotype similar to those found in the neointima of WT animals. We concluded that progressive IH was due to the effects of locally generated thrombin/PAR-1 interactions on these CD34$^+$ cells once recruited to the neointima [10]. Because this 'single-hit' mechanical injury model has few clinical counterparts, we have continued this work using mouse aortas across a full MHC mismatch (H-2^d to H-2^b) without immunosuppression, a model that involves rapid destruction of the endothelium of transplanted allografts and continuous immune-mediated damage to the donor vessel resulting in IH within 4-6 weeks [12].

Materials and methods

An expanded Methods section is available in the Online Data Supplement.

Animals and experimental models. C56BL/6 (WT) and BALB/c mice (Harlan Olac Ltd (Bicester, UK) ROSA-EYFP [13], heterozygous α-TFPI-Tg [9], homozygous PAR-1- [14] and PAR-4-deficient mice [14], were bred and maintained at Imperial College London. All have been maintained for more than 10 generations on a BL/6 background. All procedures were approved by UK Home Office.

Aortic transplantation: Mice were transplanted using a sleeve anastomosis technique[12]. Briefly, a 5mm segment of infrarenal donor aorta, flushed with heparin was transplanted into recipient aorta. Blood flow was confirmed by direct inspection after the clamps removed.

Skin transplantation: Full thickness tail skin was grafted on the lateral flanks of recipients 14 days post aortic transplantation and protected under sterile gauze covered by plaster for 9 days. Rejection was when no viable skin remained [15].

Wire-induced endoluminal carotid artery injury: This was performed as previously described [9, 10]. Briefly, a 100μm diameter wire was introduced and withdrawn three times into the common carotid via the external carotid artery before the external carotid artery was tied off. After confirming restoration of normal blood flow through the common carotid, the skin was closed and animals were allowed to recover.

Morphometric analysis and immunohistology. Sections were prepared and examined as previously described [9, 10]. For analysis of intimal and medial areas, at least three random sections were examined from each of ≥ five arteries. For immunofluorescence (IF) analysis, images were examined using the MetaMorph system (Universal Imaging, Downingtown, PA). For confocal, a Leica DM-IRBE microscope was used and images acquired using Leica TCS-NT software. Infiltration by immune cells was analysed by manual counting at x400 magnification. Average counts were derived from examination of at least six random sections from each artery. For the antibodies used, see the online data supplement.

CD34$^+$ cell separation and injection. CD34$^+$ cells were isolated as previously described [9, 10] and had an average purity of 95%**.** For comparative immunophenotyping using immunocytofluorescence, at least 300 cells were counted at X200 magnification from at least 3 random fields from 3 different wells. For functional experiments, CD34$^+$ cells were purified from mice 2-4 days after wire-induced injury, incubated in vitro for 1 hour, before 7.5 x10^5 - 1x10^6 cells were injected IV into aortic recipients 1 week post-transplantation.

Assessment of anti-donor immune responses. Anti-donor antibody (Ab) titres were assessed on donor splenocytes by flow cytometry. Circulating IFNγ was analysed by ELISA (R&D Systems). BM-derived DC were isolated and cultured as described elsewhere [16]. T cells were prepared from splenocytes and lymph node cells. Proliferation was assessed by [^{3}H]TdR incorporation.

Statistical analysis. Data are presented as means ±SEM. Significance of the difference between 2 groups was determined by unpaired Student *t* or log rank test. Values of $P<0.05$ were considered statistically significant.

Results

Phenotype of aortic transplants.

Six weeks after transplantation into C57BL/6 (H-2^b, 'WT') recipients, BALB/c (H-2^d) aortas showed florid IH with neointimal areas and neointimal/media ratios approximately 10-fold higher than those of syngeneic controls (figure 1A-C). IF of frozen sections showed widespread staining for TF co-localised with α-SMA in neointima (figure 1G). To confirm that recipient α-SMA^+ cells were TF^+ we transplanted BALB/c aortas into ROSA-EYFP mice expressing enhanced yellow fluorescent protein (EYFP) on all cells (figure 1H).
Aortas transplanted into α-TFPI-Tg mice (H-2^b) did not develop IH (figure 1D-F). IF revealed no intimal TF staining, but a rim of recipient hTFPI on the luminal aspect (figure 1I). IH did not develop when syngeneic grafts were transplanted into either strain (figures 1C and F). These data confirm that recipient α-SMA^+ TF^+ cells infiltrate the intima of transplanted vessels and that expression of hTFPI by these cells is associated with absence of IH.

Immune activation and effector mechanisms in WT vs. α-TFPI-Tg.

Titres of donor-specific, anti-BALB/c IgM and IgG Ab were similar in WT and α-TFPI-Tg recipients (Suppl figure 1A&B) as was the ***density*** of T cells, $CD68^+$ macrophages and $CD11c^+$ dendritic cells (DC) infiltrating transplanted vessels (Suppl figure 1C&D).
There were no differences in the proportions of IFNγ-secreting $CD4^+$ or $CD8^+$ T cells from spleen (Suppl figure 1E&F) or lymph nodes (Suppl figure 2A&B) in WT or α-TFPI-Tg recipients. Levels of circulating IFNγ at 2 weeks were also similar (Suppl figure 1G).
T cells and DC from each strain had a similar phenotype. Importantly, in α-TFPI-Tg mice, there was no fusion protein expressed by either cell (Suppl figure 2C&D). In vitro proliferative alloresponses to BALB/c DC by T cells from WT and α-TFPI-Tg mice were similar (Suppl figure 2E), and DC from each strain promoted similar proliferative T cell responses by allogeneic T cells (Suppl figure 2F). Finally, WT and α-TFPI-Tg recipients rejected BALB/c skin grafts at a similar tempo, even after a previous BALB/c aortic graft (Suppl figure 1H),

indicating similar alloimmune activation and effector mechanisms in both naive and sensitised mice from either strain.

Taken altogether, these data indicate that adaptive immune responses to BALB/c aortas were comparable in WT and α-TFPI-Tg mice. Therefore differences in the nature or intensity of the alloimmune injury were unlikely to account for the aortic phenotypes observed.

Adoptive transfer of $CD34^+$ cells after aortic transplantation.

Peripheral blood leukocytes were purified from WT or α-TFPI-Tg mice after endoluminal injury, separated into $CD34^+$ and $CD34^-$ fractions and injected into either WT or α-TFPI-Tg recipients 1 week post-transplantation. Endoluminal injury was used as a mechanism to enrich 'vascular progenitors' within the $CD34^+$ population [10].

The $CD34^+$, but not $CD34^-$ fractions significantly impacted on the phenotype of IH. CD34+ cells from α-TFPI-Tg mice inhibited the development of IH in WT recipients, whereas CD34+ cells from WT mice promoted IH in α-TFPI-Tg recipients (figure 2 A&B).

$hTFPI^+$ staining was detectable on the luminal aspect of the graft 2 weeks after injection of cells from α-TFPI-Tg mice (figure 2C). With cells from ROSA-EYFP mice, YFP^+ cells were seen throughout the neointima 6 weeks after injection (figure 2D). Both these results illustrate that injected $CD34^+$ cells are recruited into the allogeneic aorta.

Following our previous demonstration that hTFPI on these cells was acting to prevent thrombin generation [9, 10], $CD34^+$ cells from WT or ROSA-EYFP mice were incubated with a selective PAR-1 antagonist prior to injection. Compared to controls, these cells prevented IH (figure 2A&B). In addition, $CD34^+$ cells from PAR-1-deficient animals prevented IH (figure 2A&B). Controls from a second strain, deficient in the low affinity thrombin receptor PAR-4, also inhibited IH, but to a significantly lesser degree than cells from PAR-1 KO mice.

All these data indicate that $CD34^+$ cells have an important influence on the hyperplastic response following alloimmune injury and that inhibiting thrombin generation or PAR-1 signalling on these cells is sufficient to prevent IH.

Phenotype of endogenous circulating CD34$^+$ cells.

There was a significant increase in the number of circulating CD34$^+$ cells after transplantation (figure 3A). Beyond day 3, numbers fell rapidly back to baseline post-syngeneic transplantation but remained high after allogeneic transplantation. Cell numbers were similar in α-TFPI-Tg mice (data not shown).

TF$^+$ cells accounted for ≈75% of the CD34$^+$ cells in the circulation post-allogeneic, but only 20% post-syngeneic transplantation. Cells expressing PAR-1 made up to 50% of the CD34$^+$ cells post-allogeneic but were only a minority population post syngeneic transplantation, accounting for <10% of the CD34$^+$ cells. Finally, α-SMA$^+$ cells were found, making up ≈10% of CD34$^+$ cells in both strains post-allogeneic transplantation, but <1% cells on day 7 post-syngeneic transplantation.

Comparing the phenotype of CD34$^+$ cells in WT with those of α-TFPI-Tg mice 7 days post allogeneic transplantation, the same proportion expressed TF, PAR-1 (figure 3B), VEGFR2 α-SMA, TIE-2 and CD31, but there were significant differences in the proportion expressing CD45, CD68, F4/80, Ly6-C and CD11b (supplementary table 1). There were significant differences in the expression of these molecules by α-SMA$^+$CD34$^+$ cells (table 1). The majority in WT expressed PAR-1 alongside CD45, CD11b, CD68, F4/80, Ly-6C, CD115, CX3CR1 and CCR2 indicating they were myeloid progenitors. In addition, almost all the α-SMA$^+$ cells from WT co-expressed VEGFR-2, CD31, TIE-2 and E-selectin, suggesting an angiogenic phenotype. In contrast, the majority of α-SMA$^+$CD34$^+$ cells from α-TFPI-Tg mice were CD45-, CD11b-, CD115-, F4/80-, Ly-6C-, CX3CR1, CCR2 and PAR-1 –negative, and expressed no VEGFR-2, CD68, CD31 or E-selectin. In these mice, expression of the hTFPI fusion protein was found on both the CD45$^+$ and CD45$^-$ subpopulations, confirming that the promoter driving transgene expression was active in both lineages (figure 3C). In contrast, despite immunocytofluorescence examination of >8000 individual CD34- cells from the peripheral blood of 4 different groups of transplanted α-TFPI-Tg recipients, we detected no

α-SMA or hTFPI- expression that could not be accounted for by contaminating $CD34^+$ cells, indicating that the fusion protein was only expressed by circulating $CD34^+$ cells.

The differences between WT and α-TFPI-Tg mice were due entirely to the expression of the TFPI fusion protein, as an anti-hTFPI monoclonal Ab, injected at the time of transplantation, was associated with the appearance of significant numbers of $CD31^+$α-SMA^+ and $CD45^+$α-SMA^+ $CD34^+$ cells in these mice (Supplementary table 2). Moreover, these changes could be reversed if the Ab was administered with a PAR-1 (but not a PAR-2) antagonist (supplementary table 2) suggesting that the effect of TFPI was to inhibit signalling through PAR-1 but not PAR-2.

These data indicate profound TF and PAR-1-dependent differences between strains in the mobilisation and phenotype of $CD34^+$ cells post transplantation, with the α-TFPI-Tg mice having reduced proportions of circulating $CD45^+$ myeloid progenitors, particularly $CD45^+$α-SMA^+ cells, increased proportions of $CD45^-$α-SMA^+ cells, reduced expression of PAR-1 by α-SMA^+ cells and an absence of α-SMA $cells^+$ co-expressing VEGFR-2, CD31 and E-selectin.

Recruitment of cells to aorta after injury

To link these differences in endogenous $CD34^+$ cells to IH or repair, we studied recruitment of cells to the transplanted allografts using confocal microscopy. As previously reported[17], donor EC were rapidly lost within 24-72 hours in both WT and α-TFPI-Tg (figure 4A). In WT, new α-SMA-expressing cells were visible on the luminal aspect by day 7; these cells co-expressed CD31, CD45 and E-selectin, consistent with recruitment of the majority population of circulating $CD34^+$α-SMA^+ cells. By day 14, IH was becoming established and there was widespread expression of CD31 and CD45 throughout the neointima, with no evidence of a new endothelium being formed (figure 4).

In α-TFPI-Tg recipients, cells expressing hTFPI were detectable on the luminal aspect of the transplanted aorta by day 3 – these were $CD34^+$ but negative for CD31, CD45 (figure 5), and E-selectin (not shown), consistent with recruitment of the majority population of endogenous

$CD34^+\alpha$-SMA^+ cells in these mice. Recruitment of these cells was associated with the appearance of $CD31^+$ cells on the luminal aspect; these were also $CD34^+$ but CD45- and E-selectin-negative and appeared in areas distinct from the hTFPI-expressing cells. By day 28, a new quiescent endothelium had regenerated in the allografts transplanted into α-TFPI-Tg recipients (figure 5).

These data confirm that the α-SMA^+ cells recruited to the luminal aspect of transplanted allografts in both strains had a phenotype consistent with those of the $CD34^+\alpha$-SMA^+ cells found in the circulation.

Phenotype of mouse aortas after adoptive transfer of $CD34^+$ cells.

Aortas in WT mice injected with $CD34^+$ cells from α-TFPI-Tg were examined by IF; these developed a quiescent endothelium lacking expression of α-SMA or E-selectin (suppl figure 3A), even though the cells were injected 1 week after transplantation, at a time when recruitment of endogenous $CD45^+\alpha$-SMA^+ cells was underway. The same appearance was also seen when WT (not shown) or ROSA-EYFP $CD34^+$ cells incubated with PAR-1 antagonist (suppl figure 3C) were injected. Results from the latter indicated that injected $CD34^+$ cells contributed to the new quiescent endothelial layer, as well as the α-SMA^+ cells beneath. Finally, WT recipients injected with $CD34^+$ PAR-1-deficient cells also developed a quiescent endothelium (supplementary figure 4A), in contrast to when PAR-4-deficient cells were used (supplementary figure 4B); although IH was reduced by these cells (see figure 2), the neointima which developed had a WT appearance, with widespread staining for TF, CD31 and E-selectin.

These data indicate that thrombin or PAR-1 inhibition on $CD34^+$ cells is sufficient to promote endothelial regeneration, despite an ongoing immune response against the donor vessel and the presence of significant numbers of recipient $CD45^+\alpha$-SMA^+ progenitors circulating in these mice.

Discussion

This paper offers three novel insights into TA, by demonstrating firstly; that IH is associated with a distinct subset of $CD34^+$ $CD45^+$ α-SMA^+ cells circulating post-allogeneic transplantation whereas regenerative repair seen in α-TFPI-Tg mice is associated with a distinct subset of $CD45^-\alpha$-SMA^+ cells; secondly that IH can be prevented in the face of an aggressive anti-donor immune response by specific manipulation of thrombin generation or PAR-1 receptors on $CD34^+$ cells and finally that this manipulation promotes regenerative repair. An important point about the regenerative repair was that it occurred in the face of an aggressive immune response to the donor tissue, without specific modulation by immunosuppressive drugs.

Coagulation proteins have previously been implicated in the pathophysiology of TA, though with little understanding of the mechanisms involved. For example, chronic rejection is associated with extensive fibrin deposition within arteriosclerotic vessels in human renal allografts [18] and with widespread TF expression in rat and human cardiac allografts [19-21]. Moreover, a potent thrombin inhibitor, hirudin, has been shown to attenuate experimental TA in rat cardiac allografts [22]. Our data now provide a mechanistic explanation for the link between TF and IH, through thrombin/PAR-1 signalling on circulating $CD34^+$ cells.
PAR-1 is the archetypal member of a family of G-protein-coupled, seven transmembrane-domain cell surface receptors, designated PAR 1-4 [23-26], through which coagulation proteases mediate many of their pro-inflammatory effects. Thrombin, which cleaves PAR-1, -3 and -4 [27], influences the phenotype of numerous cell types in this way [26]. Having previously linked IH with PAR-signalling on newly recruited $CD34^+$ cells in a model of wire-induced endovascular injury [10], we now show that the same mechanism is relevant in an allogeneic transplantation model, in which the continuous immune-mediated injury is more representative of the chronic lesions seen in inflammatory vascular disease.

The immune response to transplanted aortas in α-TFPI-Tg mouse recipients was the same as in WT. Both exhibited comparable in vitro anti-donor 'direct' T cell alloresponses, stimulation of T cells by DC, production of anti-donor Ab (strongly implying comparable 'indirect' T cell activation), infiltration of the graft by macrophages, T cells and DC, and finally, rejection of H-2^d skin grafts by naïve and donor-primed animals. Others have shown that IFNγ, produced by infiltrating immune cells is the critical cytokine driving IH, as illustrated by the severely attenuated lesions developing in recipient mice lacking IFNγ [28] and importantly, the IH that develops in immunodeficient mice lacking immune cells after administration of IFNγ [29, 30]. We found that the proportion of $CD4^+$ and $CD8^+$ T cells staining for IFNγ in lymph nodes and spleen of both WT and α-TFPI-Tg recipients were similar, as was the amount of IFNγ detectable in the circulation post-transplantation. All these data strongly suggest that BALB/c grafts in either strain were subject to the same immune-mediated injury and were equally exposed to the cytokine stimulus driving IH. These findings are not surprising, considering that the α-TFPI-Tg mice do not have a systemically anticoagulated phenotype (9) and that, within the leukocyte population, the hTFPI fusion protein is expressed by only a small proportion of $CD34^+$ cells.

In their 2001 paper using the same transplantation model, utilising β-galactosidase-Tg mice, Shimizu and colleagues reported that neointimal 'SMC' were derived from the recipient BM cells rather than donor [5], a conclusion that has since been reached by others working in different models of IH [31]. These findings have remained controversial, in part because of the disputed ability of BM-derived cells to give rise to SMC and because recent publications have directly contradicted this earlier data [32, 33]. Recently, Iwata and colleagues, working in 3 separate models of IH including TA, reported significant numbers of recipient α-SMA^+ $SM22\alpha^+$ cells in the neointima, but these also expressed CD115, CD11b, F4/80 and Ly-6C, markers of the monocyte/macrophage lineage rather than established markers of differentiated SMC such as smooth muscle myosin heavy chain or calponin [8]. The authors

concluded that although BM-derived α-SMA$^+$ cells were involved in vascular remodelling, they were myeloid cells and not 'true' SMC progenitors. Our data is compatible with this work.

Moreover, we have shown that myeloid progenitors expressing markers of the 'classic' or 'inflammatory' lineage make up the majority (60-80%) of the CD34$^+$ cells mobilised by WT mice into the circulation post-transplantation, and demonstrated that some of these express α-SMA, making up nearly 10% of all CD34$^+$ cells by day 7. Many of these α-SMA$^+$ cells also expressed TIE-2, VEGFR-2, CD31 and E-selectin, indicating a haemangiocyte or vascular leukocyte lineage [34]. Although at their peak, these cells numbered no more than 30,000/ml in the circulation, these were the cells recruited to the luminal aspect of the allograft and accumulated in the expanding neointima. The co-expression of α-SMA with TF and endothelial proteins such as CD31, P-selectin and E-selectin in the neointima has been previously documented by us [10] and by other groups working in IH [35] with the luminal cells described as 'pseudoendothelial' by some [36].

These distinct CD45$^+$ α-SMA$^+$ cells were only found circulating after allogeneic and not syngeneic transplantation, suggesting that the inflammatory environment generated by the ongoing alloresponse was responsible. Although we have not addressed which mediators are involved, it is probable that IFNγ plays a role, given its established link with TA. Other features specific to allogeneic transplantation were the sustained expression of TF and PAR-1 by the majority of circulating CD34$^+$ cells.

That TF expression was relevant was demonstrated by the vessels transplanted into α-TFPI-Tg mice, which had a radically different phenotype compared to those of WT. Not only was IH inhibited, but also transplanted allogeneic vessels appeared to have undergone regenerative repair, characterised by replacement of donor endothelium with quiescent cells sitting upon a layer of new α-SMA$^+$ cells.

Although small numbers of circulating CD34$^+$ α-SMA$^+$ hTFPI$^+$ cells in these mice were CD45$^+$, the majority were predominantly CD45-, CD11b-, CD115-, F4/80-, Ly-6C-, CX3CR1,

CCR2 and PAR-1–negative and lacked expression of VEGFR-2, CD68, CD31 and E-selectin. This phenotype was directly dependent on the TFPI fusion protein. To our knowledge, this is the first description of the two subsets of α-SMA$^+$CD34$^+$ cells post-transplantation and of a link between them through coagulation proteases.

Recruitment of these cells to the allogeneic vessel wall was followed by CD34$^+$CD45-negative endothelial cells, which eventually formed a new endothelium. The same appearance was seen after adoptive transfer of purified CD34$^+$ cells from PAR-1 deficient mice and WT cells that had first been incubated with a selective PAR-1 antagonist. All these results indicate that TF was most likely the trigger to thrombin generation allowing signalling through PAR-1 and also suggested that inhibition of PAR-1 signalling on circulating CD34$^+$ cells was the most important determinant of the repair phenotype. However, the precise molecular signals resulting in the sequential recruitment of α-SMA$^+$ and CD31$^+$ cells to the allogeneic vessel are not clear.

For adoptive transfer experiments, CD34$^+$ cells were isolated from syngeneic or congenic mice that had undergone wire-induced carotid artery injury 2 days previously, so that they were enriched for CD34$^+$ cells mobilised in the context of vascular injury. We have assumed that recruitment of injected cells to the neointima is important for subsequent inhibition of IH, but cannot exclude the possibility that they also act at remote sites to influence the mobilisation or phenotype of endogenous CD34$^+$ (or other types of) cells.

In summary, this work indicates that the phenotype of alloimmune-mediated vascular injury (the phenotype of rejection) in this model is determined by the phenotype of mobilised repair cells, not by the nature of the immune response. This data should open new avenues of research into the quality and character of the endogenous repair response under conditions of ongoing inflammation. They should lead to a re-evaluation of previous data obtained from mouse models of TA and prompt a re-evaluation of the mechanisms underpinning human chronic rejection. They also have significance for the investigation and treatment of

inflammatory vascular diseases, in which more work needs to be done to explore why endogenous repair mechanisms fail to operate.

Acknowledgements.

The authors thank Prof. J. Pearson of King's College London for critical reading of the manuscript.

We acknowledge the support of the MRC Centre for Transplantation.

Sources of Funding.

The Medical Research Council, UK (award refs. G0401591 and G0801965) and the Garfield Weston Foundation supported this work.

We acknowledge additional financial support from the Department of Health via the National Institute for Health Research (NIHR) comprehensive Biomedical Research Centre award to Guy's & St Thomas' NHS Foundation Trust in partnership with King's College London and King's College Hospital NHS Foundation Trust.

Disclosures

None

References

1. Cuffy MC, Silverio AM, Qin L, Wang Y, Eid R, Brandacher G, Lakkis FG, Fuchs D, Pober JS, Tellides G. Induction of indoleamine 2,3-dioxygenase in vascular smooth muscle cells by interferon-gamma contributes to medial immunoprivilege. *J Immunol.* 2007;179:5246-5254.
2. Ensminger SM, Witzke O, Spriewald BM, Morrison K, Morris PJ, Rose ML, Wood KJ. CD8+ T cells contribute to the development of transplant arteriosclerosis despite CD154 blockade. *Transplantation.* 2000;69:2609-2612.
3. Rao DA, Tracey KJ, Pober JS. IL-1alpha and IL-1beta are endogenous mediators linking cell injury to the adaptive alloimmune response. *J Immunol.* 2007;179:6536-6546.
4. Tellides G, Pober JS. Interferon-gamma axis in graft arteriosclerosis. *Circ Res.* 2007;100:622-632.
5. Shimizu K, Sugiyama S, Aikawa M, Fukumoto Y, Rabkin E, Libby P, Mitchell RN. Host bone-marrow cells are a source of donor intimal smooth- muscle-like cells in murine aortic transplant arteriopathy. *Nat Med.* 2001;7:738-741.
6. Tanaka K, Sata M, Hirata Y, Nagai R. Diverse contribution of bone marrow cells to neointimal hyperplasia after mechanical vascular injuries. *Circ Res.* 2003;93:783-790.
7. Xu Q. Mouse models of arteriosclerosis: from arterial injuries to vascular grafts. *Am J Pathol.* 2004;165:1-10.
8. Iwata H, Manabe I, Fujiu K, Yamamoto T, Takeda N, Eguchi K, Furuya A, Kuro-o M, Sata M, Nagai R. Bone marrow-derived cells contribute to vascular

inflammation but do not differentiate into smooth muscle cell lineages. *Circulation.* 2010;122:2048-2057.

9. Chen D, Weber M, Shiels PG, Dong R, Webster Z, McVey JH, Kemball-Cook G, Tuddenham EG, Lechler RI, Dorling A. Post-injury vascular intimal hyperplasia in mice is completely inhibited by CD34+ bone marrow-derived progenitor cells expressing membrane-tethered anticoagulant fusion proteins. *J Thromb Haemost.* 2006;4:2191-2198.
10. Chen D, Abrahams JM, Smith LM, McVey JH, Lechler RI, Dorling A. Regenerative repair after endoluminal injury in mice with specific antagonism of protease activated receptors on CD34+ vascular progenitors. *Blood.* 2008;111:4155-4164.
11. Chen D, Dorling A. Critical roles for thrombin in acute and chronic inflammation. *J Thromb Haemost.* 2009;7 Suppl 1:122-126.
12. Clarke HM, Shrivastava S, Motterlini R, Sawle P, Chen D, Dorling A. Donor HO-1 expression inhibits intimal hyperplasia in unmanipulated graft recipients: a potential role for CD8+ T-cell modulation by carbon monoxide. *Transplantation.* 2009;88:653-661.
13. de Boer J, Williams A, Skavdis G, Harker N, Coles M, Tolaini M, Norton T, Williams K, Roderick K, Potocnik AJ, Kioussis D. Transgenic mice with hematopoietic and lymphoid specific expression of Cre. *Eur J Immunol.* 2003;33:314-325.
14. Connolly AJ, Ishihara H, Kahn ML, Farese RV, Jr., Coughlin SR. Role of the thrombin receptor in development and evidence for a second receptor. *Nature.* 1996;381:516-519.

15. Golshayan D, Jiang S, Tsang J, Garin MI, Mottet C, Lechler RI. In vitro-expanded donor alloantigen-specific CD4+CD25+ regulatory T cells promote experimental transplantation tolerance. *Blood.* 2007;109:827-835.

16. Lutz MB, Kukutsch N, Ogilvie AL, Rossner S, Koch F, Romani N, Schuler G. An advanced culture method for generating large quantities of highly pure dendritic cells from mouse bone marrow. *J Immunol Methods.* 1999;223:77-92.

17. Hu Y, Davison F, Zhang Z, Xu Q. Endothelial replacement and angiogenesis in arteriosclerotic lesions of allografts are contributed by circulating progenitor cells. *Circulation.* 2003;108:3122-3127.

18. Grandaliano G, Di Paolo S, Monno R, Stallone G, Ranieri E, Pontrelli P, Gesualdo L, Schena FP. Protease-activated receptor 1 and plasminogen activator inhibitor 1 expression in chronic allograft nephropathy: the role of coagulation and fibrinolysis in renal graft fibrosis. *Transplantation.* 2001;72:1437-1443.

19. Holschermann H, Bohle RM, Zeller H, Schmidt H, Stahl U, Fink L, Grimm H, Tillmanns H, Haberbosch W. In situ detection of tissue factor within the coronary intima in rat cardiac allograft vasculopathy. *Am J Pathol.* 1999;154:211-220.

20. Yamani MH, Masri CS, Ratliff NB, Bond M, Starling RC, Tuzcu EM, McCarthy PM, Young JB. The role of vitronectin receptor (alphavbeta3) and tissue factor in the pathogenesis of transplant coronary vasculopathy. *J Am Coll Cardiol.* 2002;39:804-810.

21. Yen MH, Pilkington G, Starling RC, Ratliff NB, McCarthy PM, Young JB, Chisolm GM, Penn MS. Increased tissue factor expression predicts

development of cardiac allograft vasculopathy. *Circulation.* 2002;106:1379-1383.

22. Holschermann H, Bohle RM, Schmidt H, Zeller H, Fink L, Stahl U, Grimm H, Tillmanns H, Haberbosch W. Hirudin reduces tissue factor expression and attenuates graft arteriosclerosis in rat cardiac allografts. *Circulation.* 2000;102:357-363.
23. Vu TK, Hung DT, Wheaton VI, Coughlin SR. Molecular cloning of a functional thrombin receptor reveals a novel proteolytic mechanism of receptor activation. *Cell.* 1991;64:1057-1068.
24. Nystedt S, Emilsson K, Wahlestedt C, Sundelin J. Molecular cloning of a potential proteinase activated receptor. *Proc Natl Acad Sci U S A.* 1994;91:9208-9212.
25. Ishihara H, Connolly AJ, Zeng D, Kahn ML, Zheng YW, Timmons C, Tram T, Coughlin SR. Protease-activated receptor 3 is a second thrombin receptor in humans. *Nature.* 1997;386:502-506.
26. Shrivastava S, McVey JH, Dorling A. The interface between coagulation and immunity. *Am J Transplant.* 2007;7:499-506.
27. Coughlin SR. Thrombin signalling and protease-activated receptors. *Nature.* 2000;407:258-264.
28. Raisanen-Sokolowski A, Glysing-Jensen T, Koglin J, Russell ME. Reduced transplant arteriosclerosis in murine cardiac allografts placed in interferon-gamma knockout recipients. *Am J Pathol.* 1998;152:359-365.
29. Tellides G, Tereb DA, Kirkiles-Smith NC, Kim RW, Wilson JH, Schechner JS, Lorber MI, Pober JS. Interferon-gamma elicits arteriosclerosis in the absence of leukocytes. *Nature.* 2000;403:207-211.

30. Wang Y, Bai Y, Qin L, Zhang P, Yi T, Teesdale SA, Zhao L, Pober JS, Tellides G. Interferon-gamma induces human vascular smooth muscle cell proliferation and intimal expansion by phosphatidylinositol 3-kinase dependent mammalian target of rapamycin raptor complex 1 activation. *Circ Res.* 2007;101:560-569.

31. Xu Q. Stem cells and transplant arteriosclerosis. *Circ Res.* 2008;102:1011-1024.

32. Daniel JM, Bielenberg W, Stieger P, Weinert S, Tillmanns H, Sedding DG. Time-course analysis on the differentiation of bone marrow-derived progenitor cells into smooth muscle cells during neointima formation. *Arterioscler Thromb Vasc Biol.* 2010;30:1890-1896.

33. Daniel JM, Sedding DG. Circulating smooth muscle progenitor cells in arterial remodeling. *J Mol Cell Cardiol.* 2011;50:273-279.

34. Coffelt SB, Lewis CE, Naldini L, Brown JM, Ferrara N, De Palma M. Elusive Identities and Overlapping Phenotypes of Proangiogenic Myeloid Cells in Tumors. *Am J Pathol.* 2010;178:1564-1576.

35. Sakao S, Taraseviciene-Stewart L, Cool CD, Tada Y, Kasahara Y, Kurosu K, Tanabe N, Takiguchi Y, Tatsumi K, Kuriyama T, Voelkel NF. VEGF-R blockade causes endothelial cell apoptosis, expansion of surviving CD34+ precursor cells and transdifferentiation to smooth muscle-like and neuronal-like cells. *FASEB J.* 2007;21:3640-3652.

36. Zeiffer U, Schober A, Lietz M, Liehn EA, Erl W, Emans N, Yan ZQ, Weber C. Neointimal smooth muscle cells display a proinflammatory phenotype resulting in increased leukocyte recruitment mediated by P-selectin and chemokines. *Circ Res.* 2004;94:776-784.

Figure Legends

Figure 1. IH of BALB/c aortas in WT vs. α-TFPI-Tg recipients.

Data representative of 3 independent experiments, each with 5 or 6 mice per group. IH in WT (A,B,C) vs. α-TFPI-Tg (D,E,F) recipients. Graphs (A&D) show neointimal area (left panels) and neointima:media ratio (right). Data points derived from 3 random sections from 5 different vessels. White columns = syngeneic; black = allogeneic aortas.

Elastin van Geisen staining (B&E) and brightfield images (C&F) of sections from BALB/c aortas 6 weeks post-transplantation. L; lumen. N; neointima. M; media. A; adventitia. Arrowheads demarcate the neointima.

G-I: Three colour IF of sections from 6-week BALB/c aortas. 'Co-localisation' = overlay images; yellow = co-localisation. L; lumen. N; neointima. M; media. A; adventitia. Blue = DAPI.

G: WT recipients. Red = α-SMA; Green = TF as indicated.

H: ROSA-EYFP recipients. Red = α-SMA or TF as indicated; Green = YFP. Fluorescence from the YFP has been captured through a green filter to aid co-localisation.

I: α-TFPI-Tg recipients. Red = α-SMA; Green = TF or TFPI as indicated.

Figure 2. Adoptive transfer of $CD34^-$ or $CD34^+$ cells.

Phenotypic analysis of BALB/c aortas in WT mice following adoptive transfer of 1 x 10^6 cells 1 week post-transplantation. Cells harvested from mice 2 days post- injury. N= 5 per group. Aortas harvested at 6 (A,B, &D) or 2 (C) weeks. Representative of 3 independent experiments.

A&B: Quantitative analysis of neointimal area (A) and neointima:media ratios (B). Columns show mean values ± SEM. Data points derived from 3 random sections from 5 different vessels. WT:FIIa = WT cells incubated with thrombin. WT:PAR-1 antag = WT cells incubated with PAR-1 antagonist. PAR-1/PAR-4 KO = cells from PAR-1 or 4 deficient mice.

C&D: Representative two (right) colour IF of sections (Green =hTFPI (C) or YFP (D)) after injection of cells from α-TFPI-Tg (A) or ROSA-EYFP (B) mice. L; lumen. N; neointima. M; media. A; adventitia. Blue =DAPI. Fluorescence from the YFP has been captured through a green filter to aid co-localisation.

Figure 3. Analysis of circulating CD34$^+$ cells

A: CD34$^+$ circulating in WT mice post-allogeneic (squares) or syngeneic transplantation. *p<0.05. †p<0.001 (N=6 per group)

B: Phenotype of circulating CD34$^+$ cells after allogeneic (black) or syngeneic (white) transplantation. Each graph shows the proportion of CD34$^+$ cells expressing TF, PAR-1 or α-SMA. Squares = WT; Circles = α-TFPI-Tg. In A&B, day 0 = 20 hours post-op. * p<0.05. †p<0.01 (N=6 per group)

C; Circulating CD34$^+$ cells, isolated from α-TFPI-Tg mice 7 days after BALB/c aortic transplantation, examined by immunocytofluorescence. Cells stained with hTFPI (red) and CD45 (green). Blue = DAPI. Right panel shows combined image, illustrating expression of hTFPI fusion protein by CD45+ cells (yellow arrow) and CD45- cells (red arrows).

Representative of 3 independent experiments.

Figure 4. Recruitment of cells to aortas in WT recipients

A: Three-colour immunohistological analysis of frozen sections from BALB/c aortas stained with DAPI (blue), anti-α-SMA (red) and anti-CD31 (green).

B-E: Three colour immunohistological analysis of frozen sections from allogeneic aortas harvested from WT mice. Day 0 = 20 hours post-transplantation. All sections stained with DAPI (blue) and in column: B, (red) anti-α-SMA or E-selectin as indicated: C, (green) anti-CD31 or CD45 as indicated. Column D shows overlay images. E show enlarged images from the boxed areas in D. Yellow indicates co-localisation. Rows from same day are consecutive sections.

Representative of 3 independent experiments.

Figure 5. Recruitment of cells to aortas in α-TFPI-Tg recipients

A-D: Three colour immunohistological analysis of frozen sections from BALB/c aortas transplanted into α-TFPI-Tg mice. Day 0 = 20 hours post-transplantation. All sections stained with DAPI (blue) and in column: A, (red) anti-CD31, CD34, CD45 or α-SMA as indicated: B (green) anti-hTFPI or CD31 as indicated. Column C shows overlay images. D shows enlarged images from the boxed areas in C. Yellow indicates co-localisation. Coloured arrows in images from same day are indicating the same cell in consecutive sections.

Representative of 3 independent experiments.

Table 1: Proportion of $CD34^+$ α-SMA^+ cells expressing the indicated molecules, expressed as % (±SEM) of total $CD34^+$ α-SMA^+ cells. Data derived from 6 mice.

	Phenotype of circulating $CD34^+\alpha$-SMA^+cells – Day 7		
	%(±SEM) of $CD34^+\alpha$-SMA^+cells expressing these molecules		
	WT	α-TFPI-Tg	p value
TF	100 (±0)	88 (±7.2)	NS
PAR-1	91.7 (±4.8)	9.2 (±5.8)	0.0004
VEGFR-2	81.3(±3.2)	0	0.00001
CD31	98 (±2)	0	0.000001
TIE-2	83.4 (±1.8)	59.1 (±8.2)	0.04
E-selectin	100 (±31)	0	0.03
CD45	81.7 (±5.4)	18.7 (±7.5)	0.002
CD68	69.6 (±16.1)	0	0.01
F4/80	80.2 (±6.4)	8.4 (±5.3)	0.001
Ly6-C	65.7 (±13.6)	5.4 (±2.9)	0.01
CD11b	73.9 (±7.8)	11.1 (±7.3)	0.004
CD115	71.5 (±14.7)	13.4 (±0.5)	0.02
CCR2	84.4 (±1.3)	16.9 (±3)	0.00003
CX3CR1	83.4 (±1.8)	20.8 (±4.2)	0.0002

Figure 1

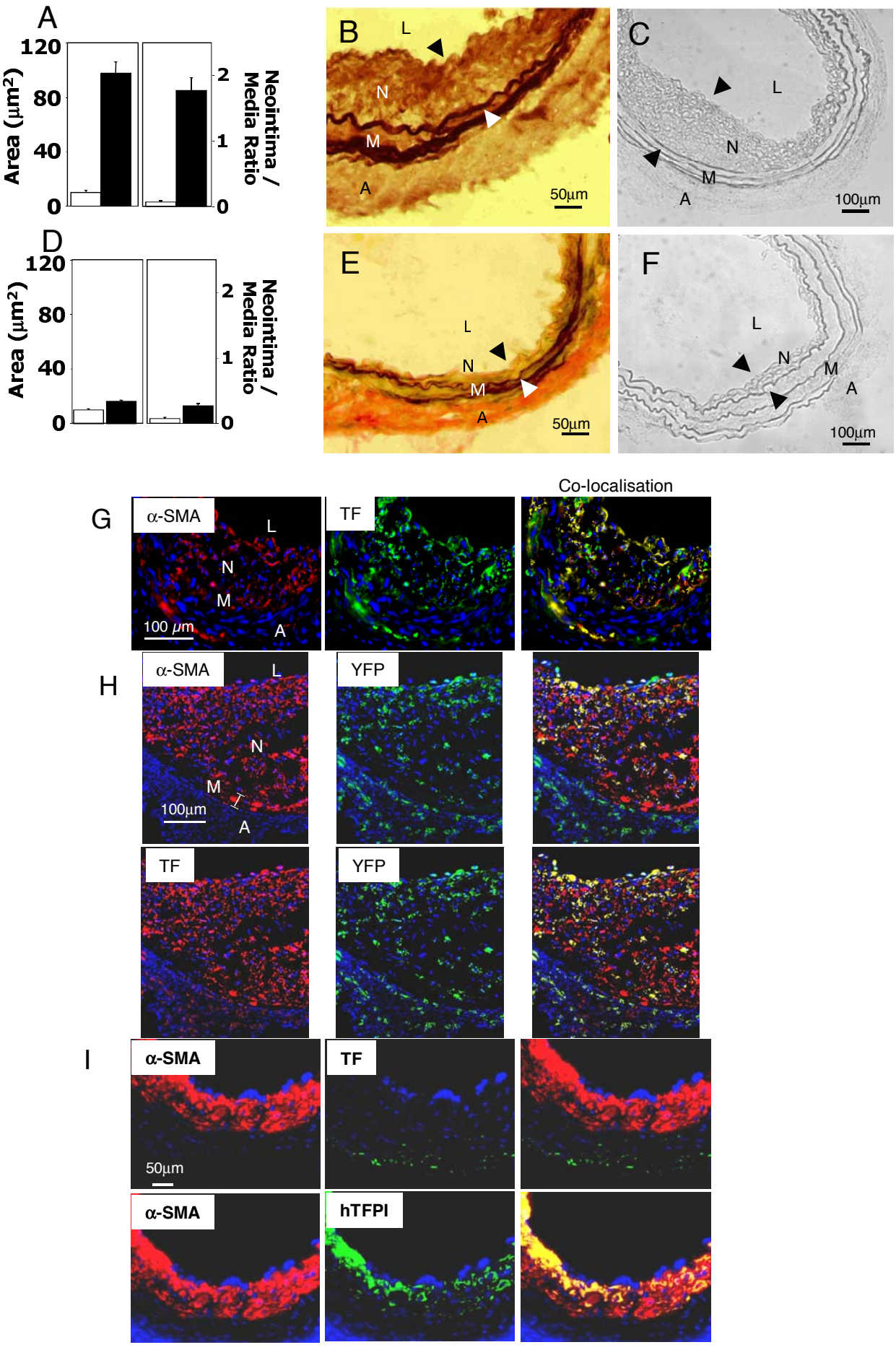

Figure 2

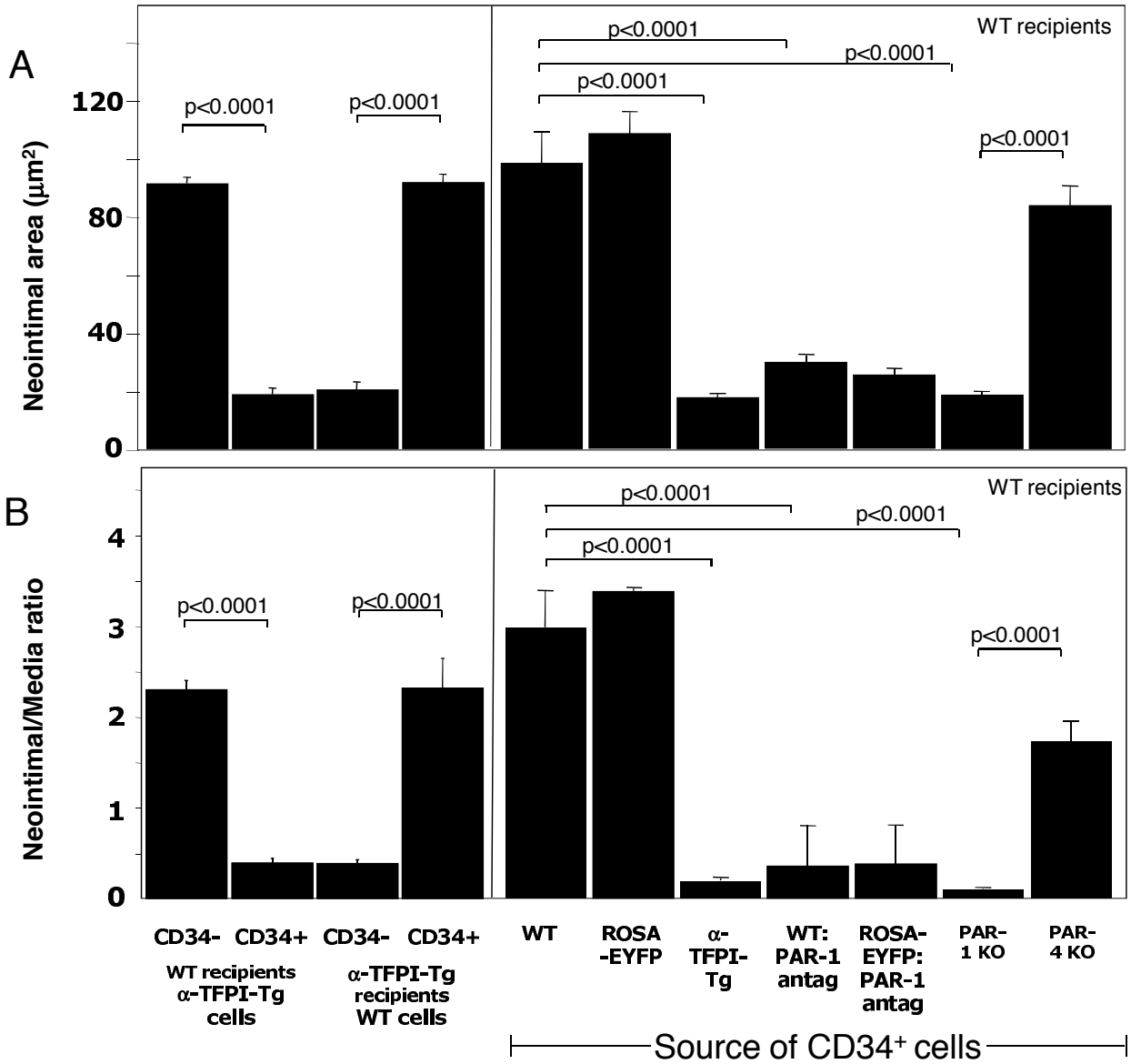

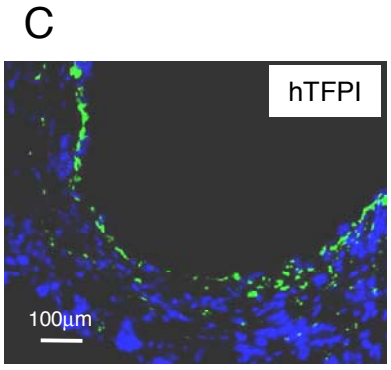

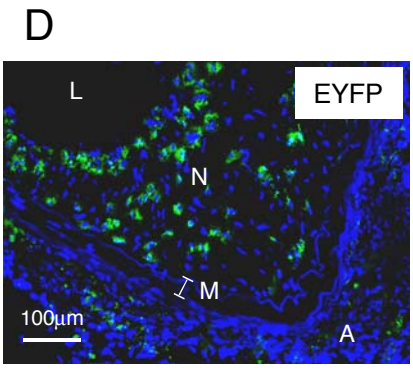

Figure 3

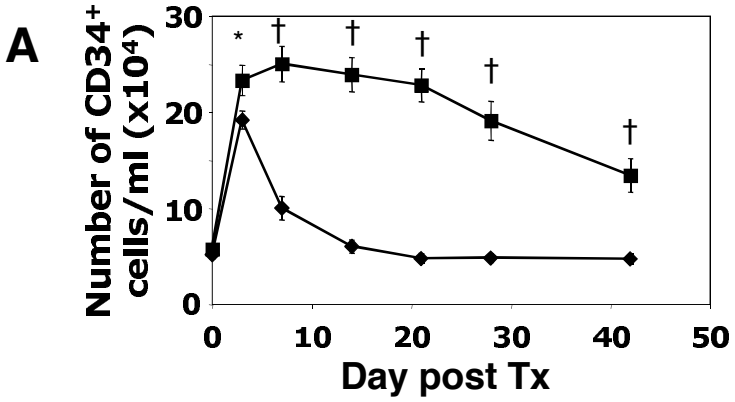

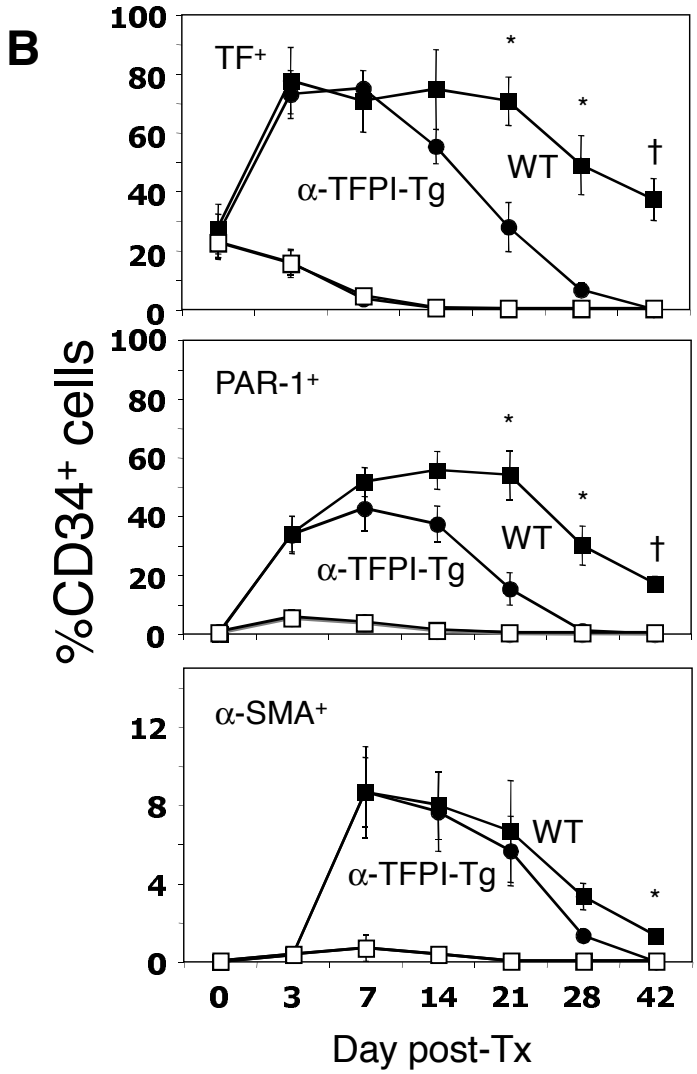

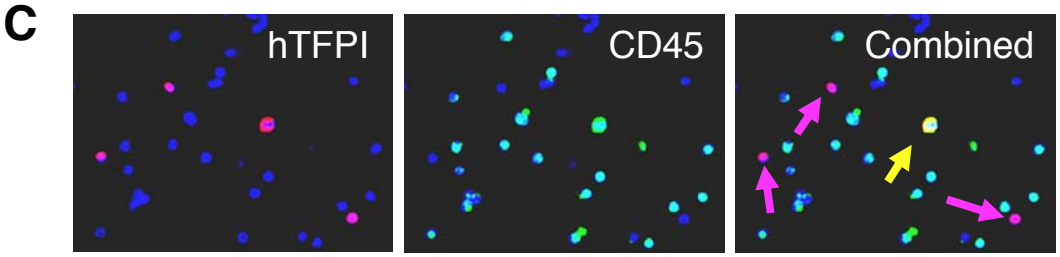

Figure 4

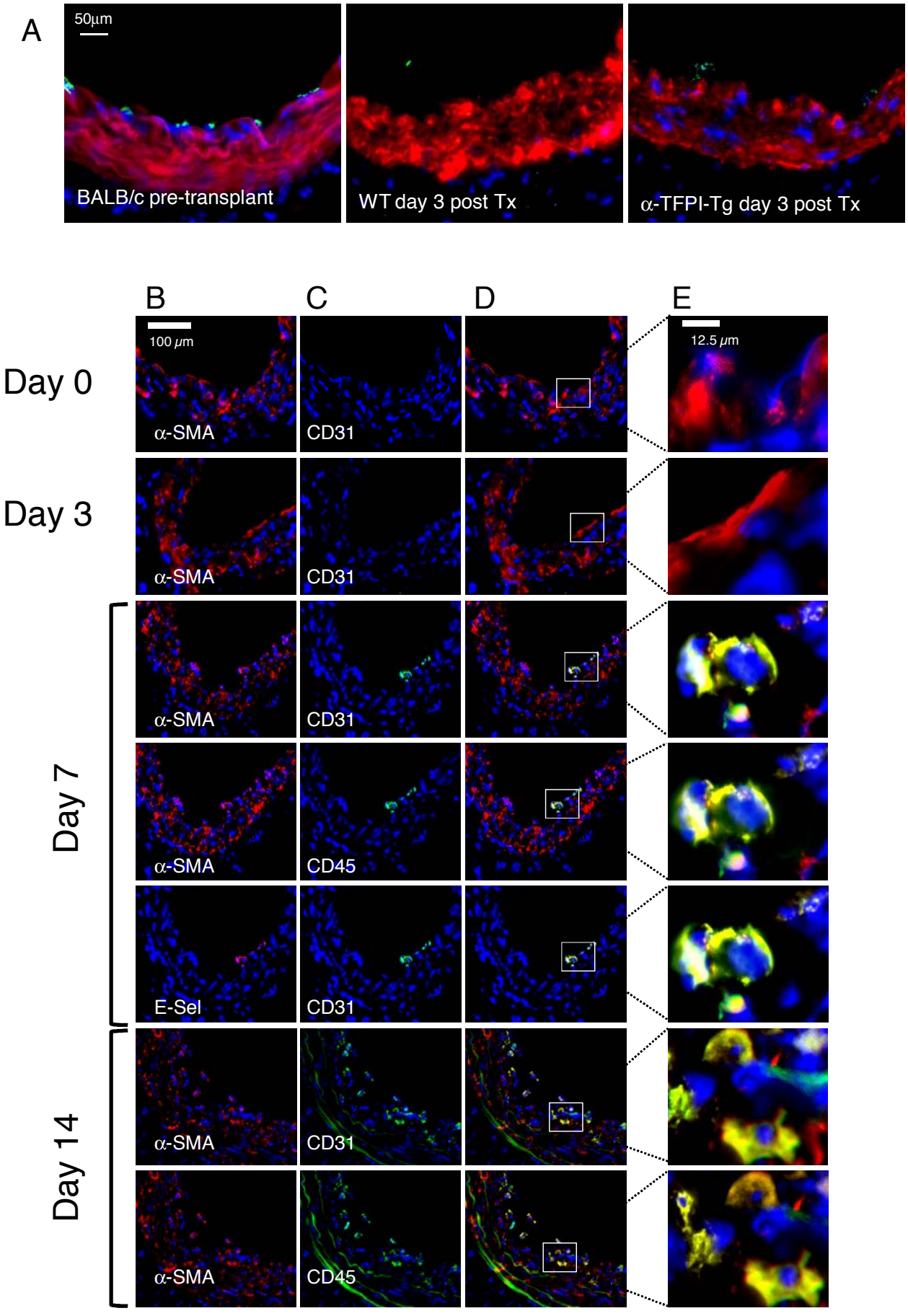

Figure 5

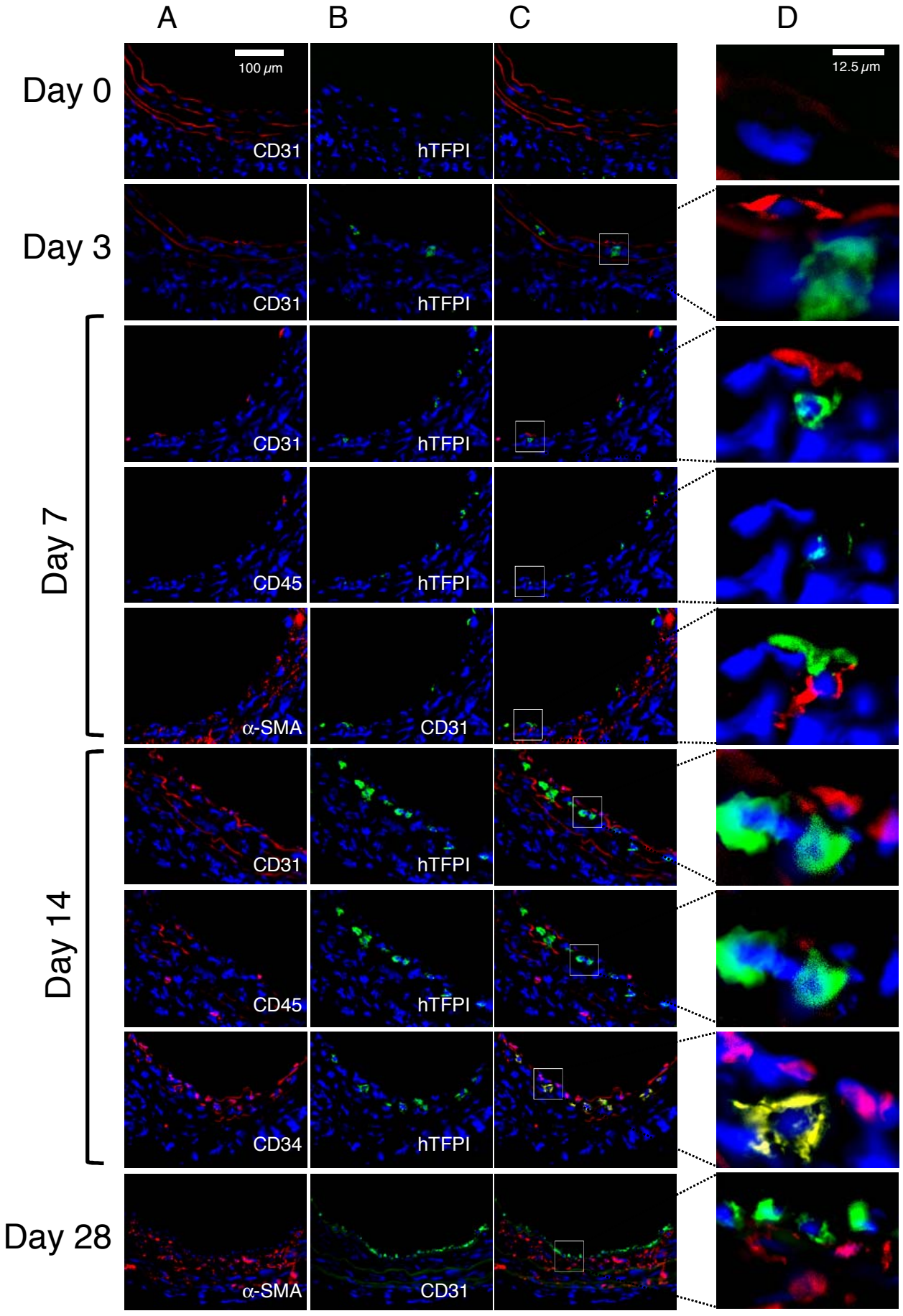

Supplemental Material

Inhibition of thrombin receptor signalling on α-smooth muscle actin$^+$ CD34$^+$ progenitors leads to repair after murine immune vascular injury.

Chen – Repair by PAR-1 inhibition on myeloid progenitors

D. Chen PhD,[1] S. Shrivastava PhD,[1,2] L. Ma PhD,[1] E-L Tham BSc,[1] J. Abrahams BSc,[2] J. D. Coe BSc, [2] D. Scott PhD, [2] R. I. Lechler PhD FRCP,[1] J. H. McVey PhD,[3] A. Dorling PhD FRCP[1]

[1] Medical Research Council (MRC) Centre for Transplantation, King's College London, King's Health Partners, Guy's Hospital, Great Maze Pond, London UK SE1 9RT

[2] Department of Immunology, Imperial College London, Hammersmith Hospital, Du Cane Road, London, UK W12 0NN

[3]Thrombosis Research Institute, Manresa Road, London, UK. SW3 6LR

Corresponding Author: Prof. Anthony Dorling, MRC Centre for Transplantation, King's College London, Guy's Hospital, London, UK SE1 9RT

Tel +44 (0)20 7188 5880 Fax +44 (0)20 7188 5660

Email; anthony.dorling@kcl.ac.uk

Detailed Materials and Methods

Animals and experimental models. WT and BALB/c mice were purchased from Harlan Olac Ltd (Bicester, United Kingdom). ROSA-EYFP [1], heterozygous α-TFPI-Tg [2] and CD31-TFPI-Tg [3], homozygous PAR-1- [4] and PAR-4-deficient mice [4] were bred and maintained in the Biological Services Unit of Imperial College London. ROSA-EYFP mice express the yellow fluorescence protein in all cells and were used to track recipient cells in the donor vessel. Mice were used at 8 – 12 weeks of age. All animal experimental procedures were approved by UK Home Office. Recovery surgery was performed using appropriate analgesia consisting either fentanyl /fluanisone ((‘Hypnorm’, 0.4 ml/kg, Janssen, Oxford, UK) in combination with midazolam (‘Hypnovel’, 5 mg/ml, Roche, Basel, Switzerland). The mixed compounds (1 part Hypnorm, 2 parts water, 1 part Hypnovel) were administered intraperitoneally at 0.1 ml/10 g. For other animals, Buprenorphine (Alstoe Veterinary, York, UK) was administered subcutaneously at a dose of 0.01 mg/Kg post-surgery (before recovery of consciousness). Animals were anesthetised by inhalation of isoflurane supply. Isoflurane vaporization for induction of anaesthesia(20-30 seconds), surgical intervention (30-40 minutes) and maintenance of anaesthesia (3.0 – 5.0 hr) were 4.0%, 1.5% and 1.0%, respectively.

Aortic transplantation: Mice were transplanted using a sleeve anastomosis technique as we have previously used [5]. Briefly, a 5mm segment of infrarenal donor aorta was removed after flushing with 300μl of N saline containing 50μl of heparin before transplantation into the same position of the recipient aorta. Blood flow was confirmed by direct inspection after the clamps removed. N=5-6 per group

Skin transplantation: Full thickness tail skin from BALB/c mice was grafted on beds prepared on the lateral flanks of recipients 14 days post aortic transplantation. Graft sites were protected under sterile gauze covered by plaster removed on day 9. Grafts

were observed daily afterward and were considered rejected when no viable skin remained [6]. Graft survival in the groups was compared using the log-rank test.

Wire-induced carotid artery injury: This was performed as we previously described [2, 7]. Briefly, a 100μm diameter wire was introduced and withdrawn three times into the common carotid via the external carotid artery before the external carotid artery was tied off. After confirming restoration of normal blood flow through the common carotid, the skin was closed and animals were allowed to recover.

Morphometric analysis and immunohistology. Sections were prepared and examined as previously described [2, 7]. Briefly, aortas were isolated and embedded in OCT (VWR International, Dorset, UK) by freezing with dry ice, sectioned at 5μm thickness and fixed in methanol at –20˚C fixed in methanol. For analysis of intimal and medial areas, sections were stained using the Accustain™ Elastin Stain kit (Sigma) and examined under an Olympus U-ULH Optical microscope (Olympus Optical Co. Ltd, Tokyo, Japan) using Image-Pro PlusTM version 3.0 software (Media Cybernetics, Silver Spring, MD, USA). At least three random sections were examined from each of five grafts / wire-injured arteries. For IF analysis, sections were examined with Plan-NEOFLUAR objectives using a KTL/CCD-1300/Y/HS camera from Princeton Instruments (Trenton, NJ). Images were analyzed using the MetaMorph imaging system (Universal Imaging, Downingtown, PA). Some images are presented as overlays on the brightfield image to highlight the position of the elastic laminae. Infiltration of aortas by recipient immune cells was analysed by manual counting at x400 magnification. At least six random sections from each graft were measured, and average counts calculated.

Progenitor cell separation and injection. Whole mouse blood was collected 2-3 days post-injury. $CD34^+$ cells were isolated using a stem cell separation kit according to the manufacturer's instructions (Stemcell Technology, London, UK). The average purity of the $CD34^+$ cell populations was approximately 95% as assessed by flow cytometry**.** For comparative immunophenotyping using immunocytofluorescence,

$CD34^+$ cells were plated into a 24 well plate at $5x10^3$ cells/well, centrifuged at 1000 rpm, fixed with 4% paraformaldehyde (PFA), washed with PBS for 3 times, centrifuged at 1800 rpm for 2 min and then labelled with one or more of the Ab as listed below. For some analyses, fixation occurred *after* first layer staining. All wells were stained with DAPI. Labelled cells were analyzed using an immunofluorescence microscopy (Axiovert S100 TV; Zeiss, Welwyn Garden City, UK). To determine subpopulation densities, at least 300 cells were counted at X200 magnification from at least 3 random fields from 3 different wells.

For functional experiments, $CD34^+$ cells were purified from mice 2-4 days after injury, seeded in a 24-well plate at $2x10^4$ cells /ml and cultured in Iscove's MDM (Sigma) supplemented with 2% FBS (Stemcell Technology) for 1-5 days. Cells were incubated with either thrombin (Enzyme Research Laboratories Ltd, Swansea, UK) or inactive thrombin (Cambridge Bioscience, Cambridge, UK), both at 50nM, Mercaptopropionyl-Phe-Cha-Arg-Lys-Pro-Asn-Asp-Lys-NH2 (PAR-1 antagonist) or Trans-cinnamoyl YPGKF-NH2 (PAR-4 antagonist) (both from Peptides International Inc. Louisville, KY 40224, USA) at 10μM.

$7.5\ x10^5$ -$1x10^6$ freshly prepared $CD34^+$ cells were injected into aortic recipients through a tail vein 1 week post-transplantation. In some experiments, cells were cultured in either medium, 500nM thrombin or 10μM PAR-1 antagonist for 1 hour, before injection.

Ab for IF or immunocytofluorescence. The Ab used were monoclonal rat anti-mouse CD34, CD68 (Serotec, Oxford, United Kingdom), and CD31, CD3, CD4, CD8 (BD Bioscience Pharmingen, Oxford, United Kingdom); polyclonal rabbit anti–TF, VEGF-R2 (ABR-Affinity BioReagents,Golden, CO), SM22α, P-selectin (BD Bioscience Pharmingen), anti-PAR 1 and anti-PAR 4 (Autogenbioclear, Wiltshire, UK) and human TFPI (American Diagnostica, Stamford, CA, USA); mouse

monoclonal anti-PAR 2[1] (Zymed, California, USA) and anti–human α-SMA (Sigma-Aldrich, St Louis, MO, USA); chicken anti–mouse E-selectin (R&D Systems, Minneapolis, MN, USA); hamster anti-mouse CD11c (Serotec). Second layer staining was with either goat anti-rat IgG-FITC, goat anti-rabbit IgG-FITC, sheep anti-mouse IgG-FITC or rabbit anti–chicken IgG-FITC (all from Sigma-Aldrich), rabbit anti-hamster IgG-FITC (BD Biosciences), or horse anti-mouse IgG–Texas red (Vector Laboratories, Burlingame, CA, USA). Sections were counterstained with DAPI for three colour IF. For human sections the following were used; FITC-labelled sheep anti-human VWF (Serotec), CD31 (Antibodies GmbH, Aachen, Germany) and TF (Affinity Biologicals, Ancaster, Canada), mouse anti-human E-selectin [8] or Cy3-labelled mouse anti-α-SMA (Sigma).

Assessment of anti-donor Ab and circulating cytokines. Blood was obtained from euthanized recipient mice 2 weeks post-transplantation by cardiac puncture, diluted with one-tenth volume of 3.2% sodium citrate and spun at 250g for 5 minutes at 4°C to isolate plasma, which was stored at –80°C until used. For assessment of anti-donor Ab, spleens from BALB/c mice aged 6 to 10 weeks were minced and passed through a 70μm nylon cell strainer (BD Bioscience, Bedford, MA, USA) before digestion in 0.2% collagenase D (Boehringer Mannheim, Germany) in DMEM medium at 37°C for 30 minutes. Red blood cells were lysed using ACK buffer. The remaining cells were suspended in PBS/BSA at $1x10^6$ cells/ml, incubated with mouse Seroblock FcR (AbD Serotec, Oxford, UK) for 10 min at RT and then with serial dilutions of the recipient mouse plasma for 1 hour at RT. After three brief washes in PBS, cells were incubated with either goat anti-mouse IgG or IgM (Sigma, UK) for 1 h at 4°C in the dark. As a negative control, cells were stained with plasma from a non-transplanted mouse. Flow cytometric analysis was performed as described below.

[1] Anti-PAR reagents recognize both cleaved and non-cleaved forms of the receptor.

Circulating IFNγ was analysed by enzyme-linked immunosorbent assay (ELISA) (from R&D Systems) according to the manufacturer's instructions.

Immune activation assays. BM-derived DC were cultured as described elsewhere [9]. Briefly, BM cells were flushed out from the femurs and tibiae of mice and passed through a nylon cell strainer. Red blood cells were lysed using ACK buffer. After washing, cells were seeded in tissue culture flasks or plates at concentration of $1x10^6$/ml in RPMI growth medium plus 2.5% supernatant from granulocyte-macrophage colony-stimulating factor (GM-CSF) producing hybridoma cell line. On day 3, non-adherent cells were discarded and fresh medium was added. On day 6, half the medium (plus non-adherent cells) was removed from culture and discarded. Fresh RPMI growth medium with 1.25% GM-CSF hybridoma supernatant was added back to the rest of the culture. On day 6, 1μg/ml LPS (Escherichia coli serotype 0128:B12, Sigma) or 1μM dexamethasone (Sigma) was added to the culture medium for 24 hours to produce strongly or poorly immunogenic DC respectively. Cells were harvested on day 8.

For co-culture assays, splenocytes and lymph node cells (mesenteric and axillary) were prepared as above. To enrich for T cells, cell suspensions underwent 2 rounds of adherence for 45 minutes onto plastic culture flasks at 37˚C. Non-adherent cells were incubated with the following monoclonal Ab; anti-MHC II (M5114), anti-CD16/32 and anti-CD45R (B220; all from eBioscience, Insight, Wembley, UK) with or without anti-CD8 or anti-CD4 (BD Pharmingen). T cells were negatively selected using sheep-anti-rat magnetic beads (Dynal). To assess proliferation, stimulator cell proliferation was inhibited with γ-irradiation. Plates were pulsed with [^{3}H]TdR for 18 hours (overnight) on day 5. Proliferation was measured as [^{3}H]TdR incorporation by liquid scintillation spectroscopy.

Flow cytometric analysis was performed on a FACSCalibur flow cytometer and analysed using Cellquest (BD BioSciences, UK) or Flojo (Treestar, USA) software.

$2x10^5$ cells were washed in PBS containing 5% heat inactivated FCS then stained with the appropriate concentration of Ab (see above) in buffer in 96 well V-bottom plates and incubated for thirty minutes in the dark at 4°C. After three washes, they were stained with a relevant secondary Ab before further washing. Cells were analysed immediately or fixed in 2% paraformaldehyde for analysis within three days. For intracellular cytokine staining, splenocytes or lymph node cells were isolated as above and stimulated with PMA (Sigma) at 50ng/ml plus ionomycin (Calbiochem) at 500ng/ml for 4 hours. Brefeldin A (Sigma) was added at 10ng/ml for the last 2 hours of incubation. Cells were washed and incubated with rat anti-mouse CD4-APC (BD Pharmingen). Following further washing, cells were fixed in 2% paraformaldehyde for 20 minutes at room temperature then washed. Cells were permeabilised by incubating in PBS 5% FCS with 0.5% saponin (Sigma) for 10 minutes, and then stained with rat anti-mouse IFN-γ-FITC (BD Pharmingen) and washed thoroughly prior to analysis by flow cytometry**.**

Statistical analysis. Data are presented as means ±SEM. Significance of the difference between 2 groups was determined by unpaired Student *t* or log rank test. Values of $P<0.05$ were considered statistically significant.

Supplemental References

1. de Boer J, Williams A, Skavdis G, Harker N, Coles M, Tolaini M, Norton T, Williams K, Roderick K, Potocnik AJ, Kioussis D. Transgenic mice with hematopoietic and lymphoid specific expression of Cre. *Eur J Immunol.* Feb 2003;33:314-325.

2. Chen D, Weber M, Shiels PG, Dong R, Webster Z, McVey JH, Kemball-Cook G, Tuddenham EG, Lechler RI, Dorling A. Post-injury vascular intimal hyperplasia in mice is completely inhibited by CD34+ bone marrow-derived progenitor cells expressing membrane-tethered anticoagulant fusion proteins. *J Thromb Haemost.* 2006;4:2191-2198.

3. Chen D, Giannopoulos K, Shiels PG, Webster Z, McVey JH, Kemball-Cook G, Tuddenham E, Moore M, Lechler R, Dorling A. Inhibition of intravascular thrombosis in murine endotoxemia by targeted expression of hirudin and tissue factor pathway inhibitor analogs to activated endothelium. *Blood.* Sep 1 2004;104:1344-1349.

4. Connolly AJ, Ishihara H, Kahn ML, Farese RV, Jr., Coughlin SR. Role of the thrombin receptor in development and evidence for a second receptor. *Nature.* Jun 6 1996;381:516-519.

5. Clarke HM, Shrivastava S, Motterlini R, Sawle P, Chen D, Dorling A. Donor HO-1 expression inhibits intimal hyperplasia in unmanipulated graft recipients: a potential role for CD8+ T-cell modulation by carbon monoxide. *Transplantation.* Sep 15 2009;88:653-661.

6. Golshayan D, Jiang S, Tsang J, Garin MI, Mottet C, Lechler RI. In vitro-expanded donor alloantigen-specific CD4+CD25+ regulatory T cells promote experimental transplantation tolerance. *Blood.* Jan 15 2007;109:827-835.

7. Chen D, Abrahams JM, Smith LM, McVey JH, Lechler RI, Dorling A. Regenerative repair after endoluminal injury in mice with specific antagonism

of protease activated receptors on CD34+ vascular progenitors. *Blood.* Apr 15 2008;111:4155-4164.

8. Wellicome SM, Thornhill MH, Thomas DS, Pitzalis C, Lanchbury JSS, Haskard DO. A monoclonal antibody that detects a novel antigen on endothelial cells that is induced by tumour necrosis factor, IL-1 or lipopolysaccharide. *J. Immunol.* 1990;144:2558.

9. Lutz MB, Kukutsch N, Ogilvie AL, Rossner S, Koch F, Romani N, Schuler G. An advanced culture method for generating large quantities of highly pure dendritic cells from mouse bone marrow. *J Immunol Methods.* Feb 1 1999;223:77-92.

Supplementary Figure Legends

Supplementary Figure 1. Adaptive immune response in WT (white symbols/columns) vs. α-TFPI-Tg (black) recipients.

A&B: Flow cytometric analysis of circulating anti-BALB/c Ab in serum from day 14 assessed by binding to BALB/c splenocytes (A). Data points represent means (± SEM) from 5 individual mice. Comparing WT vs. α-TFPI-Tg, p=NS all dilutions. Profiles from single mouse (B) showing binding of specific serum diluted 1 in 4. Control serum from non-transplanted mouse.

C: Analysis of $CD4^+$, $CD8^+$, $CD68^+$ and $CD11c^+$ cells infiltrating adventitia and neointima at 6 weeks. Graphs show mean density (± SEM) of 18 counts, obtained from 3 random sections from each of 6 recipients. At least 100 cells per section were counted. Comparing WT vs. α-TFPI-Tg, p=NS all comparisons.

D: Two colour IF (overlayed on brightfield) of representative sections. $CD4^+$, $CD8^+$, $CD68^+$ and $CD11c^+$ cells (all green). Red = α-SMA.

E&F: Flow cytometric analysis of (E) $CD4^+IFN\gamma^+$ (F) $CD8^+IFN\gamma^+$ cells purified from spleens of recipient mice 2 weeks post-transplantation. Data points represent individual mice. Inverted triangles, syngeneic grafts; squares, BALB/c grafts. In both, *p<0.05; **p=NS.

Similar data for LN cells are presented in supplementary figure 2.

G: Mean ± SEM IFNγ levels in peripheral blood (n=5). Each sample tested in duplicate by ELISA. Squares –syngeneic grafts. Circles –BALB/c grafts. Comparing allograft recipients, p=NS at all time points.

H: Survival of BALB/c skin grafts transplanted 2 weeks post-aortic transplantation. Inverted triangles –syngeneic aortas. Squares, BALB/c aortas. Comparing allograft recipients, p=NS at all time points.

Supplementary Figure 2. Additional data on the adaptive immune responses in WT (white symbols/columns) vs. α-TFPI-Tg (black) mice.

A & B: Flow cytometric analysis of (A) $CD4^+IFN\gamma^+$ (B) $CD8^+IFN\gamma^+$ cells purified from lymph nodes of mice 2 weeks post-transplantation. Data points represent individual mice, with mean shown by horizontal line. Inverted triangles = recipients of syngeneic grafts. Squares, recipients of BALB/c grafts. In both, *p<0.03; **p=NS. [NB *some* data from WT mice in B have been presented before in HM Clarke et al, Transplantation **88**, 653 (Sep 15, 2009)]

C & D: Flow cytometric analysis of resting and activated CD4+T cells (C) and DC (D) from WT and α-TFPI-Tg mice. Filled-in profiles = isotype control.

E&F: Functional analysis of $CD4^+$ T cells (E) and DC stimulatory capacity (F). Results are expressed as mean cpm +/- SEM after ^{3}H-thymidine uptake by 2 x 10^5 recipient (E) or BALB/c (F) $CD4^+$ T cells in triplicate wells after 5 day culture with BALB/c (E) or recipient (F) BM-derived LPS-activated DC.

Supplementary Figure 3. Immunohistology after adoptive transfer $CD34^+$ cells

Phenotypic analysis of BALB/c aortas transplanted in WT mice with adoptive transfer of 1 x 10^6 $CD34^+$ cells. N=5 mice per group. All aortas harvested at 6 weeks. Some IF images have been overlayed on the brightfield image to illustrate elastic laminae. 'Co-localisation' = two (left column) and three (right column) colour overlay images, where yellow = co-localisation. Blue = DAPI.

A: $CD34^+$ cells from α-TFPI-Tg mice. Red = α-SMA; Green = TF, P-selectin (P-sel), CD31 or E-selectin (E-sel) as indicated.

B: $CD34^+$ cells from EYFP mice, incubated in vitro with PAR-1 antagonist. Red = TF, CD31 or E-selectin (E-sel) as indicated; Green = YFP.

Supplementary Figure 4. Immunohistology after adoptive transfer $CD34^+$ cells

Phenotypic analysis of BALB/c aortas transplanted in WT mice with adoptive transfer of 1 x 10^6 $CD34^+$ cells. N=5 mice per group. All aortas harvested at 6 weeks. Some IF images have been overlayed on the brightfield image to illustrate elastic laminae. 'Co-localisation' = two (left column) and three (right column) colour overlay images, where yellow = co-localisation. Blue = DAPI.

A: $CD34^+$ cells from PAR-1-deficient mice. Red = α-SMA; Green = TF, P-selectin (P-sel), CD31 or E-selectin (E-sel) as indicated.

A: $CD34^+$ cells from PAR-4-deficient mice. Red = α-SMA; Green = TF, P-selectin (P-sel), CD31 or E-selectin (E-sel) as indicated.

Supplementary Table I: Proportion of CD34+ cells expressing the indicated molecules, expressed as % (±SEM) of total $CD34^+$ cells. Data derived from 6 mice

	Phenotype of circulating $CD34^+$ cells – Day 7		
	% (±SEM) of $CD34^+$ cells expressing these molecules		
	WT	α-TFPI-Tg	p value
TF	71 (±9)	74 (±6)	NS
PAR-1	52 (±5)	43 (±8)	NS
VEGFR-2	84 (±7)	73 (±9)	NS
α-SMA	9.4 (± 0.7)	9.6 (±0.7)	NS
CD31	26 (±6)	27 (±5)	NS
TIE-2	70 (±4)	62 (±6)	NS
E-selectin	25 (7.8)	2 (0.7)	0.04
CD45	68 (±5)	36 (±4)	0.0006
CD68	44 (±9)	2 (±1)	0.01
F4/80	46 (±6)	25 (±4)	0.05
Ly6-C	58 (±6)	29 (±5)	0.02
CD11b	63 (±7)	33 (±6)	0.03
CD115	63 (±10)	35 (±7)	0.09
CCR2	64 (±4)	53 (±5)	NS
CX3CR1	70 (±4)	58 (±6)	NS

Supplementary Table II: Proportion of $CD34^+$ α-SMA^+ cells in α-TFPI-Tg mice expressing the indicated molecules, expressed as % (±SEM) of total $CD34^+$ α-SMA^+ cells. Data from 6 mice.

	Phenotype of circulating $CD34^+$ cells – Day 7 %(±SEM) of $CD34^+\alpha$-SMA^+cells expressing these molecules						
	With control Ig	With anti-TFPI	P value	With anti-TFPI + PAR-1 agonist	P value (vs. anti-TFPI)	With anti-TFPI + PAR-2 agonist	P value (vs. anti-TFPI)
CD45+	14.3 (±3)	74.5 (±6)	0.01	21.8 (±8)	0.006	65.5 (±11)	NS
CD31+	0	86.4 (±1)	<0.001	14 (±2)	<0.001	76 (±10)	NS

Supplementary figure I

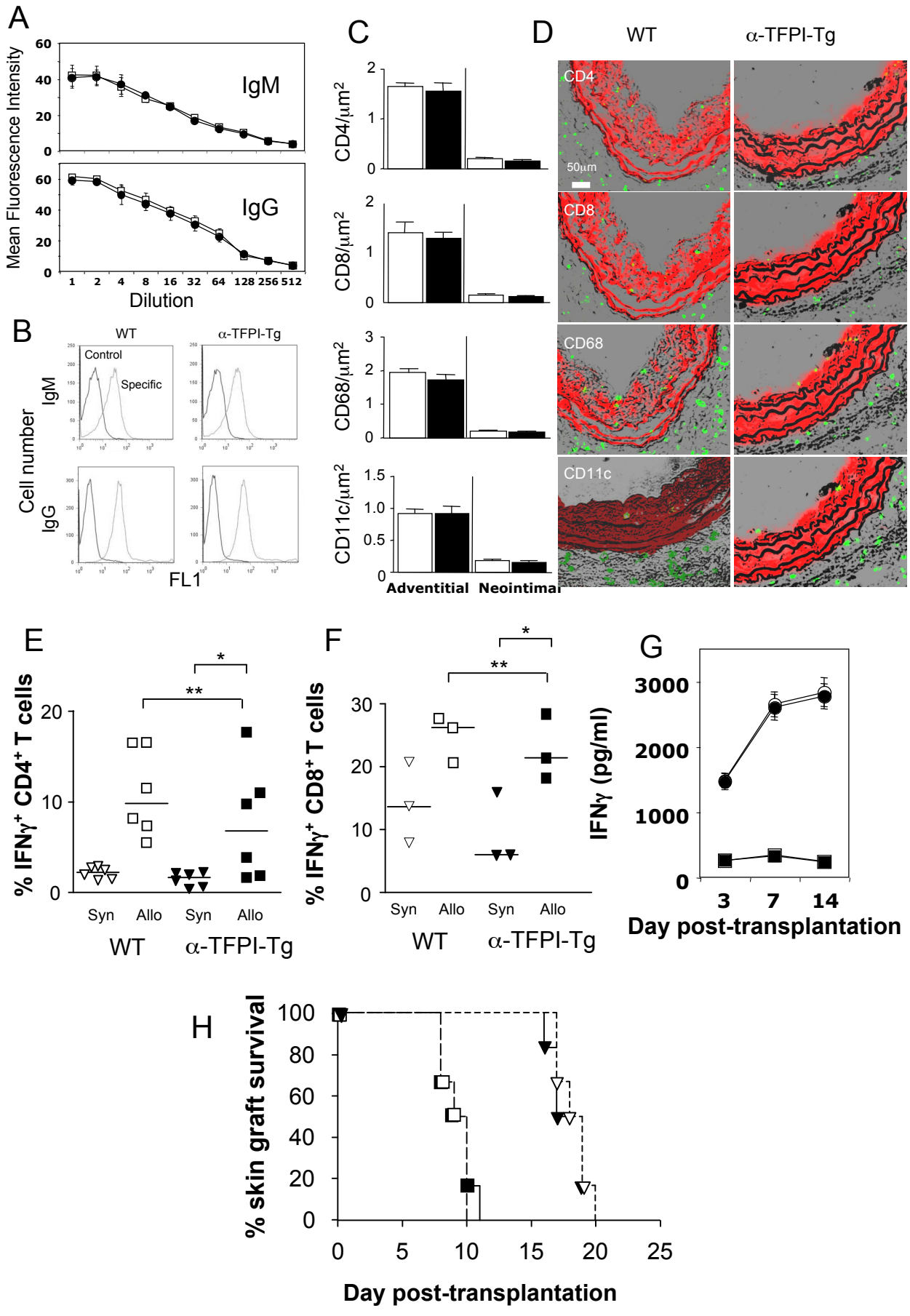

Supplementary figure II

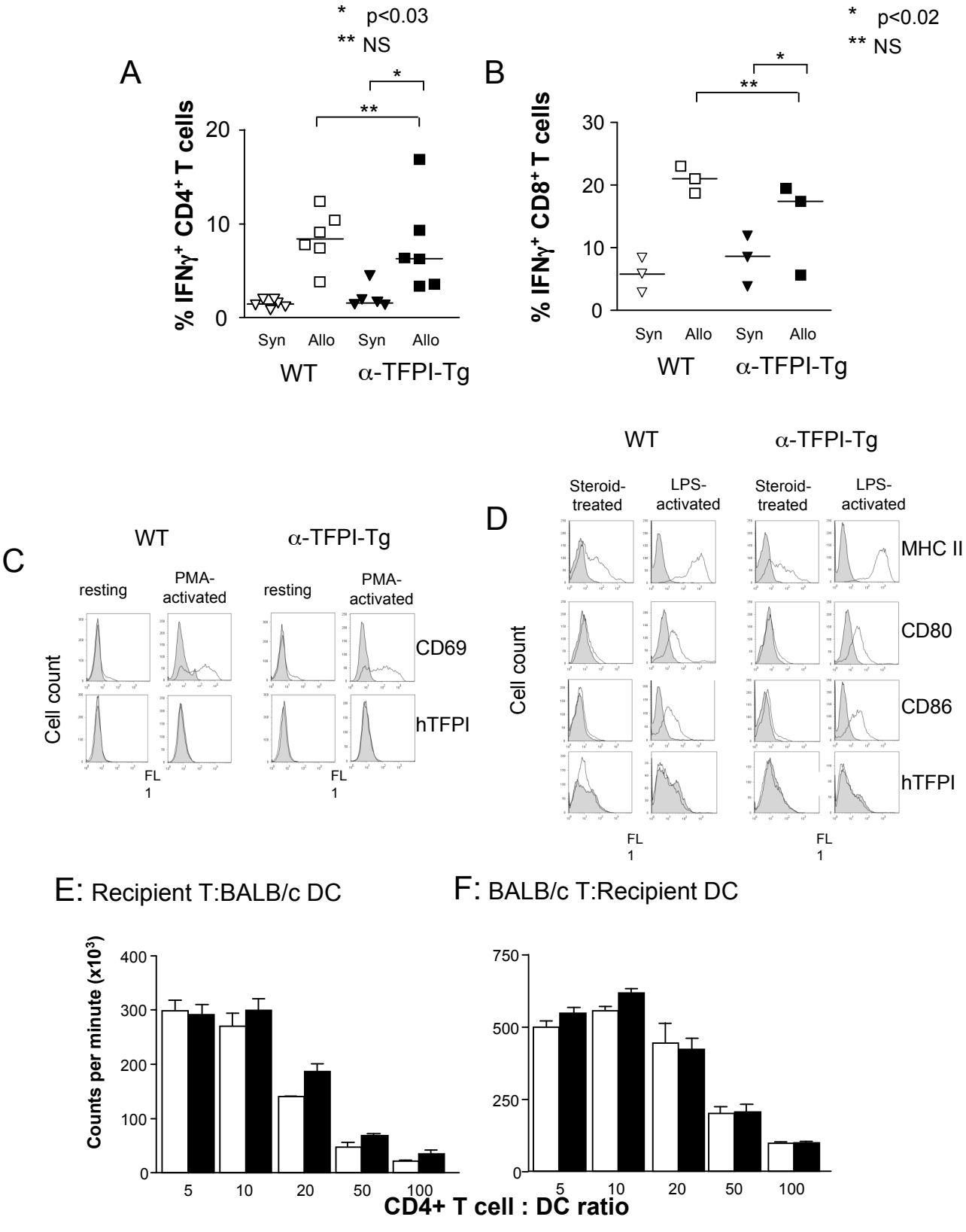

Supplementary Figure III

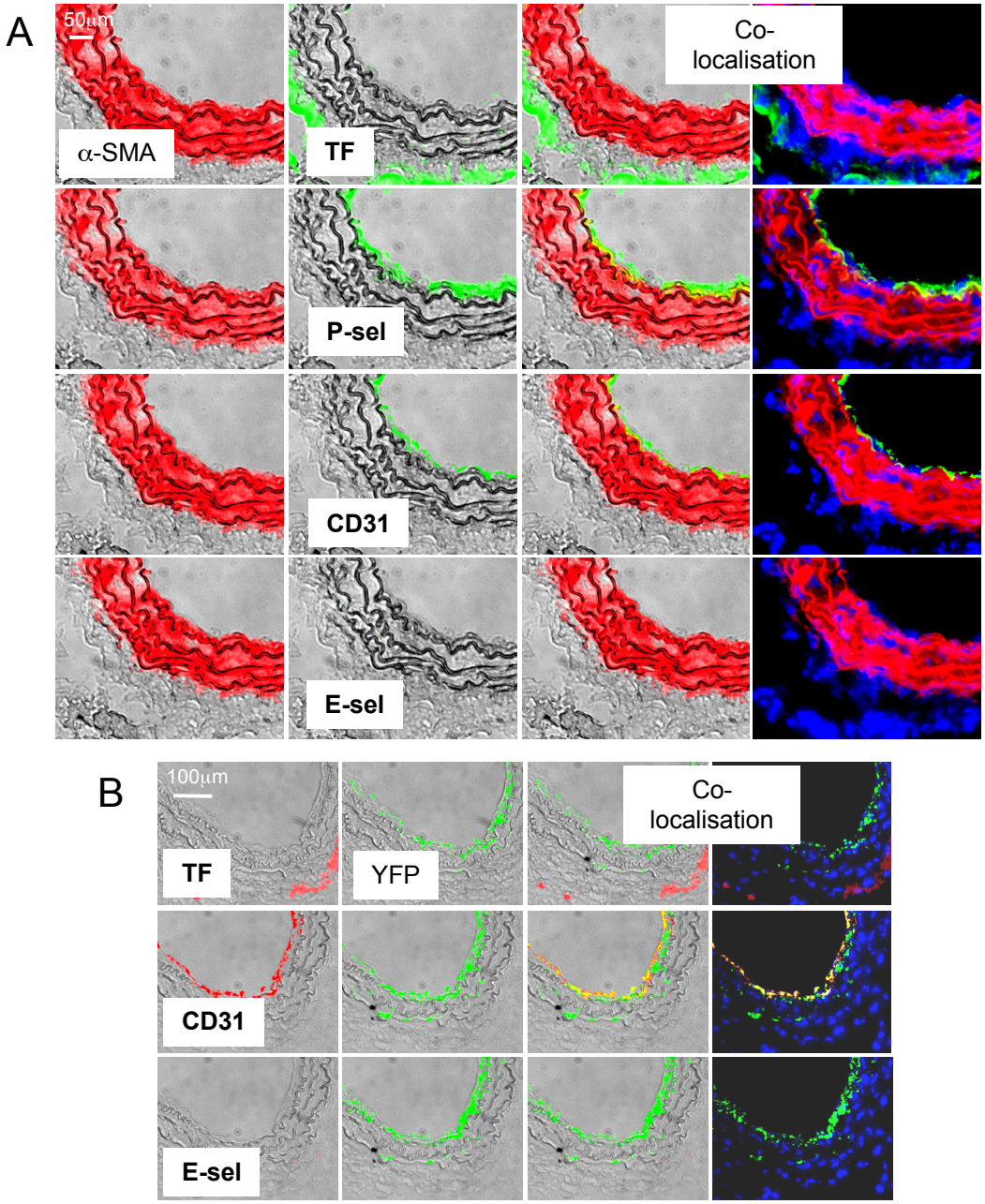

Supplementary Figure IV